Tunable spectral interferometry for broadband phase detection by use of a pair of optical parametric amplifiers

Dmitriy Panasenko,* Sergey Putilin, and Yeshaiahu Fainman

Department of Electrical and Computer Engineering, University of California, San Diego, 9500 Gilman Drive, La Jolla, California 92093-0407

Received June 18, 2004; revised manuscript received November 16, 2004; accepted November 18, 2004

We demonstrate tunable, single-pulse spectral phase measurement of broadband ultrafast signals by linear spectral interferometry. The approach is based on a coherently coupled pair of optical parametric amplifiers (OPAs). The first amplifier is the source of a signal pulse that is coupled into a nonlinear medium, where the pulse generates a broadband signal by nonlinear interactions; the second OPA provides a phase-correlated reference pulse that can be tuned across the broad spectral range and used for complete characterization of the broadband signal generated by the first OPA. An experimental demonstration of the technique for a nonlinearly modulated femtosecond pulse with a bandwidth of >200 nm occupying the range 1.13–1.36 μm is given.

OCIS codes: 320.0320, 320.7100, 190.4970.

1. INTRODUCTION

Nonlinear interactions of ultrashort laser pulses with transparent dielectric materials have been the subject of intensive research for the past few decades. Spectral broadening of intense femtosecond pulses propagating in the nonlinear regime has attracted much attention both in terms of a fundamental understanding of light–matter interaction[1–3] and for various applications such as ultrashort-pulse generation,[4–6] optical communications, and nonlinear signal processing.[7–9] Spectral broadening with generation of broadband continuum light (supercontinuum) has found important applications in frequency metrology, biomedical imaging, and atmospheric sensing.[10–12]

Experimentally, the analysis of nonlinear interactions of ultrashort pulses usually requires the means to characterize the electric field (i.e., amplitude and phase) of ultrafast optical waveforms. The techniques that are of particular importance for the characterization of nonlinear effects are those that perform the characterization by using a single shot (single exposure) of the detector and, potentially, the characterization of a single pulse in a periodic pulse train.[13,14] The importance of these properties arises from the extreme sensitivity of nonlinearly generated signals to noise and to pulse-to-pulse parameter fluctuations in the input waveform. Slight fluctuations in the input signal can be significantly amplified because of the presence of a high degree of nonlinearity, and this would result in erroneous experimental measurements if a multishot technique, for which the result is an average over a large number of laser pulses, were used.

In general any single-shot technique is inherently more power consuming than a multishot technique, as it relies on spreading the laser beam in at least one spatial dimension to permit faster parallel detection with a detector array. Additionally, the investigation of nonlinear interactions frequently requires using a wide range of input power levels to identify different processes that contribute to formation of the output signal. These factors limit the application of single-shot nonlinear techniques that use second-harmonic generation, the Kerr effect, or nonlinear absorption.[13–15]

Spectral interferometry[16] uses linear detection of interference between the spectra of the signal pulse, $s(t)\exp(i\omega_c t)$, and of the reference pulse, $r(t+\tau)\exp[i\omega_c(t+\tau)]$, with a relative time delay [here $s(t)$ and $r(t)$ are complex amplitudes of the signal and the reference, respectively]

$$I(\omega) = |\tilde{s}(\omega-\omega_c)|^2 + |\tilde{r}(\omega-\omega_c)|^2 + |\tilde{s}(\omega-\omega_c)||\tilde{r}(\omega-\omega_c)|\exp\{i[\varphi_s(\omega-\omega_c) - \varphi_r(\omega-\omega_c) + \omega\tau]\} + \text{c.c.}, \quad (1)$$

where $\tilde{s}(\omega-\omega_c)$ and $\tilde{r}(\omega-\omega_c)$ are complex Fourier amplitudes of the signal and the reference with phases φ_s and φ_r, respectively. The spectral phase information is carried by the last term in Eq. (1); the first two terms constitute the dc component. Measurement of $I(\omega)$ provides the difference between the spectral phases of the signal and the reference pulses $\varphi_s(\omega-\omega_c) - \varphi_r(\omega-\omega_c)$. Therefore, when the spectral phase of the reference pulse is known the reconstruction of the spectral phase of the signal becomes a straightforward task. The measurement of the spectral intensity can easily be achieved with the same setup, thus permitting complete characterization of the electric field of the signal pulse.

In conventional spectral interferometry the signal and the reference pulses are derived from the same ultrafast source.[17,18] The output is split into two beams. One beam is coupled into the nonlinear medium, while the other beam is unaltered and serves as a reference. Fre-

quently the phase of the reference is left unknown and only the difference between the spectral phases of the output laser pulse and the pulse that exhibits nonlinear interaction is detected. This phase difference, however, allows the nonlinear phase that is acquired by the signal during propagation to be detected. Alternatively, the reference pulse can be characterized and later its spectral phase can be taken into account during reconstruction.[19]

Spectral interferometry has been extensively applied to the analysis of nonlinear interactions with femtosecond laser pulses.[17,18] However, the conventional approach in which signal and reference are derived from the same laser source is restricted to investigation of the nonlinear effects of moderate strength. As can be seen from Eq. (1), the reference pulse must have the same spectral support as the signal pulse, which limits the spectral bandwidth that can be detected. More generally, one must have a reference for all the frequencies that are present in the signal, which is not possible if the signal exhibits significant spectral broadening.

In this paper we describe a novel approach to spectral interferometry that permits broadband-tunable single-pulse detection of the spectral phase of signals that exhibit nonlinear interactions and consequent spectral broadening. The essence of the approach lies in using an independently tunable reference pulse that is derived from a separate laser source. For the two independent sources to be correlated in spectral phase, which is necessary for measurement of interference, we use a pair of optical parametric amplifiers (OPAs) pumped by the same ultrafast amplified laser system. The pulse from the first OPA is used as a signal that propagates in a nonlinear medium, whereas the pulse from the second OPA is used as a tunable reference signal. To characterize the broad bandwidth of the signal we create multiple spectral interferograms, using several shots of the output signal interfered with a sequence of reference pulses centered at different wavelengths, ultimately covering the whole nonlinearly generated bandwidth of the output signal. Processing each spectral interferogram provides a section of the spectral phase function centered at the reference wavelength and limited to the reference bandwidth. We reconstruct the full spectral phase function by joining these sections. (The details of the reconstruction are presented in Section 4 below).

It should be noted that, whereas this approach does not permit acquisition of the whole spectral phase in a single shot, each individual measurement is performed by use of a single laser pulse. Should the spectrum and the phase of the signal exhibit fluctuations, the fluctuations can be easily identified. Moreover, by recording an ensemble of interferograms for each wavelength and monitoring input intensity, the output spectrum, or both, we can find matching sets of measurements and use them for phase reconstruction.

To demonstrate the method we experimentally characterize the spectral phase of a ~200-fs pulse that exhibited almost three-fold spectral broadening after being focused into 2-cm glass window. In our experiments we employ a modification of the spectral interferometry approach that uses two-dimensional spectral interferograms. The modified approach has the advantage of providing intuitive visual information about the spectral phase (a two-dimensional interferogram can be considered essentially a graph of spectral phase versus frequency).

In Section 2 we briefly review the two-dimensional spectral interference approach. In Section 3 we describe details of the experimental setup. Section 4 is devoted to reconstruction of the full spectral phase function from a set of interferograms with the reference pulse centered at a different wavelength. Experimental results of the detection of a nonlinearly generated signal with a bandwidth of 1.13–1.36 mm are described in Section 5, and a summary and conclusions are presented in Section 6.

2. TWO-DIMENSIONAL SPECTRAL INTERFEROMETRY

A two-dimensional spectral interferogram[20–24] (or digital spectral hologram) approach is a modification of spectral interferometry that allows intuitive visual access to the spectral phase. It was applied previously to measurement of the spectral phase of ultrashort laser pulses[20,21,23] as well as to measurement of the group delay of optical components[22] and space–time coupling in ultrashort pulses.[24] Conventional spectral interferometry described by Eq. (1) uses a relative time delay τ between the signal and the reference pulses to introduce a temporal carrier frequency used for separating the interferometric signal that carries the phase from the dc term $|\tilde{s}(\omega - \omega_c)|^2 + |\tilde{r}(\omega - \omega_c)|^2$. In contrast, the digital hologram approach (see Fig. 1) utilizes a spatial rather then a temporal carrier frequency. The spatial carrier is introduced in the direction perpendicular to the direction of the spectral decomposition (the reference beam is propagating at an angle in a vertical direction relative to the signal beam). A cylindrical lens performs a Fourier transform in the x coordinate while it leaves free-space propagating beams in the y direction. The spatial field distribution in the Fourier-transform plane of a spectral decomposition device (back focal plane of the lens in Fig. 1) is a Fourier transform of the input temporal signal scaled to the spatial coordinates.[25] Thus we can represent a two-dimensional field distribution in the plane of the photodetector array as

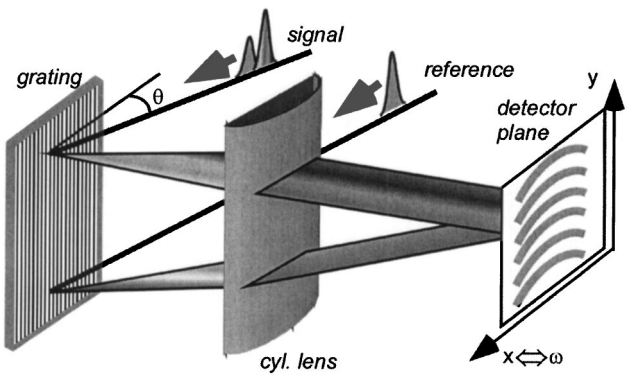

Fig. 1. Two-dimensional spectral interferometry approach to broadband phase detection. The carrier frequency is introduced in the vertical direction (y axis) by propagation of the beams at a relative angle.

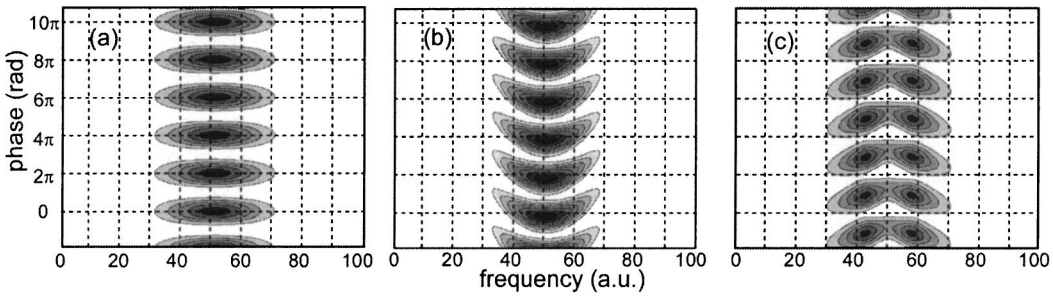

Fig. 2. Modeled spectral interferograms showing spectral interference between a transform-limited Gaussian reference pulse and a Gaussian signal pulse that possesses various phase modulations: (a) transform-limited pulse, (b) linearly chirped pulse, (c) pulse with self-phase modulation.

$$E_{\mathrm{det}}(x, y) = \tilde{s}(\kappa x)\exp[-i(\omega_s - \kappa x)t] + \tilde{r}(\kappa x)\exp[-i(\omega_r - \kappa x)t]\exp(ik_y y), \quad (2)$$

where $\kappa = -2\pi c/\sin(\theta)\lambda f$, θ is the diffraction angle, f is the focal distance of the lens (see Fig. 1), and k_y is a spatial frequency determined by the relative angle between the reference and the signal beams. The detected intensity pattern is therefore given by

$$H = |\tilde{s}(\kappa x)|^2 + |\tilde{r}(\kappa x)|^2 + |\tilde{s}(\kappa x)||\tilde{r}^*(\kappa x)| \times \exp[-i(\varphi_s(\kappa x) - \varphi_r(\kappa x) - k_y y)] + \text{c.c.} \quad (3)$$

We observe that Eq. (3) has the same form as Eq. (1), with the spectral phase of the signal given by the argument of the interferometric term carried by spatial frequency k_y. The interference occurs in the y direction (Fig. 1), creating a two-dimensional pattern. The shape of the fringes directly displays the spectral phase of the signal, as illustrated in Fig. 2, where examples of simulation of spectral interferograms for signal pulses that possess various types of phase modulation are shown. The single fringe shape of the interferogram can be considered a graph of the spectral phase versus frequency. The scaling of the y axis is determined by the 2π fringe period.

The spectral phase-reconstruction procedure from a digital hologram is similar to that for a one-dimensional interferogram. The two-dimensional Fourier transform of the hologram will contain components centered at zero frequency and at $\pm k_y$. The spectral phase is the argument of the inverse Fourier transform of one of the two terms centered at $\pm k_y$ that is selected by digital filtering. The spatial carrier needs to be chosen to ensure separation of interferometric signals and the dc term.

3. EXPERIMENTAL SETUP

A schematic diagram of the experimental setup is shown in Fig. 3. We use two OPAs pumped by the commercial Ti:sapphire regenerative amplifier delivering 100-fs pulses at a wavelength of 800 nm with energy of 1 mJ per pulse and a repetition rate of 1 kHz. Each OPA is seeded by a separate white-light continuum generated by focusing pump radiation onto 3-mm-thick sapphire plates. Signal and idler waves are generated in 3-mm-long β-barium borate crystals. Wavelength tuning is achieved by control of phase matching by rotation of the nonlinear crystal. In the study described here we utilized signal pulses from both OPAs in the range 1.1–1.4 μm. An important property of such a double-OPA system is that, although separate white-light continua are used as a seed, the generated pulses are phase correlated with each other and will interfere.[26] The pulse from the first OPA is coupled into the nonlinear medium, while the pulse from the second OPA serves as a tunable reference. A pulse shaper at the output of the second OPA is used to compensate for a residual chirp and to create a transform-limited reference pulse. In fact, the previous investigation[15] demonstrated that the pulse from the OPA has rather small nonlinear modulation, so we simply used a shift of the output diffraction grating to compensate for the residual linear chirp (the required shift was small enough not to induce an appreciable spatial chirp). If a nonlinear phase has to be compensated for, a well-developed pulse-shaping approach with spatial light modulators can be utilized.[27]

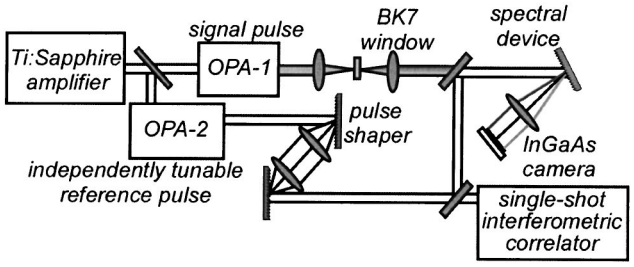

Fig. 3. Experimental system for tunable spectral phase measurement by use of a pair of OPAs.

The shape of the reference pulse was controlled in real time by a single-shot interferometric correlator.[28] A representative correlation of the reference pulse at a wavelength of 1222 nm is shown in Fig. 4(a). Figure 4(b) illustrates the phase-modulation test: good overlap of the pulse intensity autocorrelation with the second-harmonic field correlation shows that the pulse is nearly transform limited.[29]

The spectral interferogram was detected by an InGaAs infrared camera with a resolution of 252×316. We achieved single-pulse detection of the interferogram by setting the camera's integration time to 1 ms, corresponding to a 1-kHz repetition rate of the laser. The camera is capable of operating in a movie mode to record an ensemble of interferograms with subsequent analysis and comparison of the individual frames.

4. RECONSTRUCTION OF SPECTRAL PHASE FROM MULTIPLE INTERFEROGRAMS

As described in Section 1, our approach to broadband spectral phase detection is based on recording several spectral interferograms, with each interferogram corresponding to the reference pulse tuned to a different wavelength. Therefore each interferogram contains information about the spectral phase of the signal within the bandwidth of the reference pulse. This concatenation allows the wide bandwidth that is generated when a signal pulse exhibits strong nonlinear interaction to be covered. Reconstruction of the full spectral phase function requires joining together the piecewise spectral phase information obtained from the different interferograms. We do this by using overlapping portions of the reference spectra as described below.

Frequency tuning of the reference pulse is achieved by angular rotation of the nonlinear crystal in the OPA. Unfortunately during this procedure the optical path of the beam in the nonlinear crystal changes both because of a geometrical factor and as the result of a change in the refractive index of the birefringent material in the direction of beam propagation. Therefore the absolute time delay between the pulses from the two OPAs will change when the reference pulse OPA is tuned between two distinct frequencies. This time delay results in a relative linear phase factor between the spectral interferograms that corresponds to different reference wavelengths and has to be taken into account to accurately reconstruct the full spectral phase across the signal bandwidth.

Additionally, in our experiments the interference patterns that correspond to different shots of the laser fluctuate with time, most probably because of mechanical instabilities. The fluctuations produce a constant phase shift between the phases extracted from different interferograms.

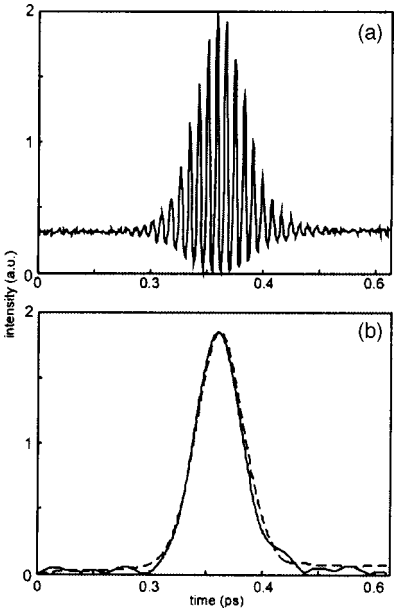

Fig. 4. (a) Interferometric correlation of the reference pulse at a wavelength of 1222 nm after compensation for residual chirp. (b) Intensity autocorrelation (solid curve) and second-harmonic field correlation (dashed curve) extracted from the correlation trace of (a) by filtering zero and high-frequency components, respectively. The good overlap of the two curves indicates the absence of phase modulation in the pulse.

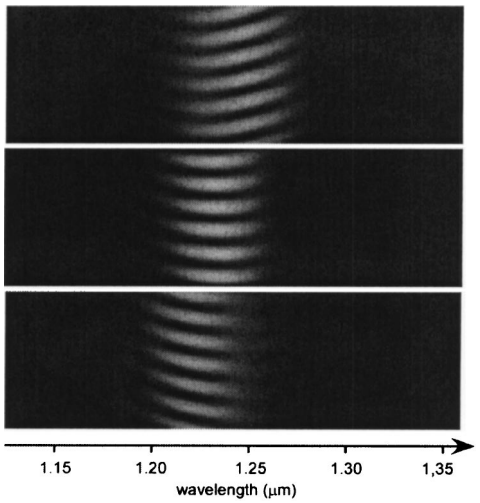

Fig. 5. CCD snapshots of the spectral intererograms of the signal pulse with the reference pulse centered at (top to bottom) 1259, 1253, and 1248 nm.

To account for these factors in reconstruction of the full spectral phase, we record a set of interferograms with the frequency shift of the reference spectrum small enough to permit overlap between two consecutive interferograms. The overlapping regions are used to eliminate the linear phase and phase shifts, thus permitting reconstruction of the complete spectral phase function.

For an initial test of the spectral phase reconstruction from multiple interferograms we characterized the pulse in the output of the signal OPA, using three spectral positions of the pulse from the reference OPA. Figure 5 shows CCD snapshots of the three independently detected interferograms, which correspond to the reference pulse tuned to three distinct center wavelengths. The parabolic shape of the fringes indicates the presence of linear chirp in the pulse. We processed each interferogram independently to extract the spectral phase, which we differentiated to obtain the group delay. The group delay was assumed to be continuous at the points where data from different holograms were joined.

A continuous group-delay function is obtained by addition of constant values to the group delays from different interferograms to produce equal values in the overlapping regions of the spectra. The group delay is then integrated back to produce the spectral phase shown in Fig. 6 together with the spectral intensity. We detect the spectral intensity simply by blocking the reference channel after the phase measurement has been performed. The spectral regions that correspond to the data from different interferograms are shown shaded. The obtained complex spectrum was inverse Fourier transformed, and an intensity autocorrelation of the pulse was calculated for comparison with the correlation measured with the single-shot correlator. Figure 7 illustrates excellent agreement between the two independent results, proving the validity of our phase-reconstruction method. The reconstructed spectral phase is close to a quadratic function

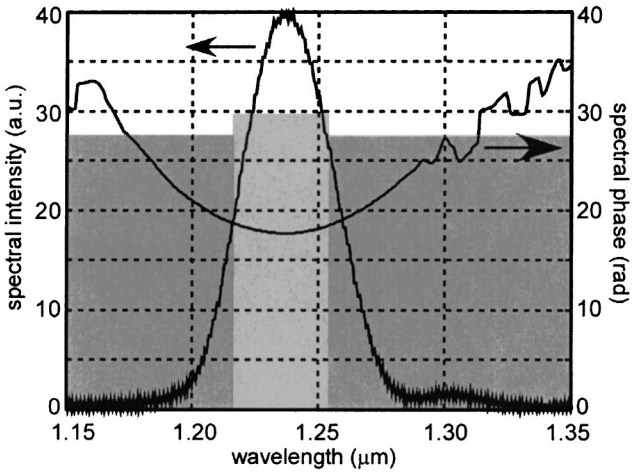

Fig. 6. Spectrum and spectral phase of the signal pulse reconstructed from the three interferograms of Fig. 5. We eliminated the unknown linear phase between the interferograms by assuming continuity of the group delay. The shaded areas show the data that correspond to three different interferograms.

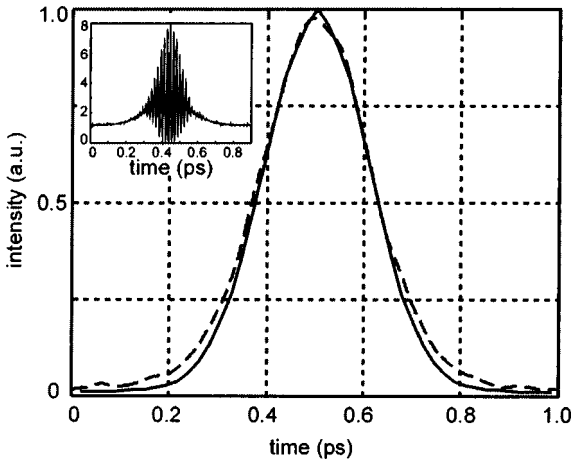

Fig. 7. Comparison of the intensity autocorrelation calculated with the reconstructed electric field of the signal pulse (solid curve) and those measured with a single-shot interferometric correlator (dashed curve). Inset, the interferometric correlation trace, which has a shape that is typical for a linearly chirped pulse, in agreement with the quadratic shape of the phase function in Fig. 6.

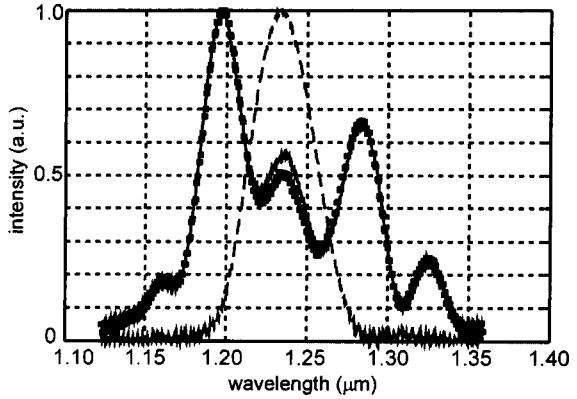

Fig. 8. Spectral intensity of a nonlinearly modulated pulse at the center (solid curve) and on the edge (squares) of the spatial mode. The slight difference between the two curves indicates that the modulation is spatially variant. The input signal's spectrum is shown by a dashed curve.

(linearly chirped pulse), which also matches the characteristic shape of the interferometric correlation shown in the inset of Fig. 7.[30]

It should be noted that, although the continuity of the group delay is an assumption that might not necessarily be fulfilled across the whole bandwidth of the signal, in practice the group-delay continuity is required only at the points where the multiple interferograms are joined together. As a two-dimensional interferogram essentially represents a plot of the spectral phase versus frequency, the discontinuities in the group delay can easily be identified visually, and these regions can be avoided when one is selecting points for joining the independently acquired interferograms.

5. EXPERIMENTAL RESULTS

To demonstrate the application of our approach to the study of nonlinear effects we investigated the spectrum generated by a signal pulse at 1230 nm focused into a 2-cm-thick BK7 glass window by using a 50-mm lens. Taking the nonlinear refractive index of BK7 glass to be $n_2 = 2.8 \times 10^{-20}\,\mathrm{m^2/W}$,[31] we calculated the critical power for the self-focusing to be $P_{\mathrm{crit}} = (0.61\lambda)^2\pi/(8n_0n_2) = 5.4\,\mathrm{MW}$. The equivalent cw power of the input pulses was ~2 mW, corresponding to an energy per pulse of a 2×10^{-6} J and to 10-MW peak power for a pulse width of 200 fs. For these parameters of the input pulse, significant spectral broadening was observed (see Fig. 8). In general, the amount of modulation is spatially dependent (the on-axis beam exhibits stronger modulation) because of self-focusing. We used an aperture after the collimating lens to select the central part of the beam. The spatial effect in the remaining part of the beam is fairly negligible, as shown in Fig. 8, where the spectral intensity at the center of the mode is compared with that at the edge of the mode. The average standard deviation of the spectral intensity corresponding to the different shots of the laser lay within 5%. We therefore considered the generated signal to be quasi-stationary, i.e., steady enough that we can use different shots of the laser without normalization to the input power.

Figure 8 shows that the generated signal exhibits almost threefold spectral broadening compared with the bandwidth of the input pulse, shown by a dashed curve in Fig. 8. In addition to broadening in the near IR, weak blue light was generated that we believe resulted from multiphoton absorption.

In our experiment we recorded 11 interferograms that correspond to the different positions of the reference wavelength (see the caption to Fig. 9). Three representative interferograms are shown in Fig. 10. Group delays reconstructed from the interferograms are shown in Fig. 9. Note that overlapping portions of adjacent group-delay curves are parallel as expected and can be used to eliminate unknown linear phase factors that come from the temporal delay of the reference as well as a constant phase shift caused by mechanical instability. Each group-delay function has noisy regions that correspond to the parts of the signal spectra that do not overlap the reference. The constant shift between the curves in Fig. 9 was introduced for the sake of illustration.

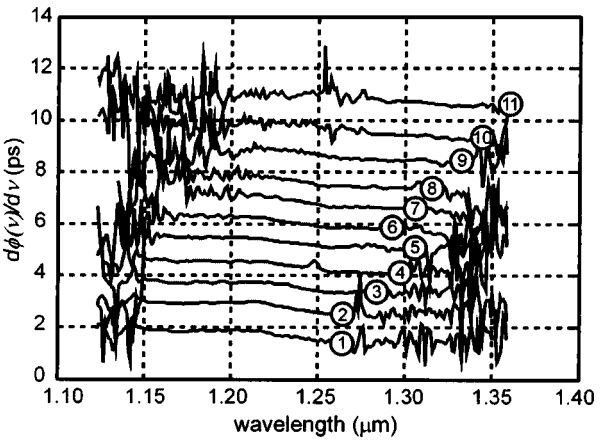

Fig. 9. Reconstructed group delays for different positions of the reference spectrum. The central wavelengths of the references that correspond to the curve numbers are 1, 1189 nm; 2, 1207 nm; 3, 1212 nm; 4, 1235 nm; 5, 1248 nm; 6, 1259 nm; 7, 1270 nm; 8, 1282 nm; 9, 1295 nm; 10, 1305 nm; 11, 1315 nm.

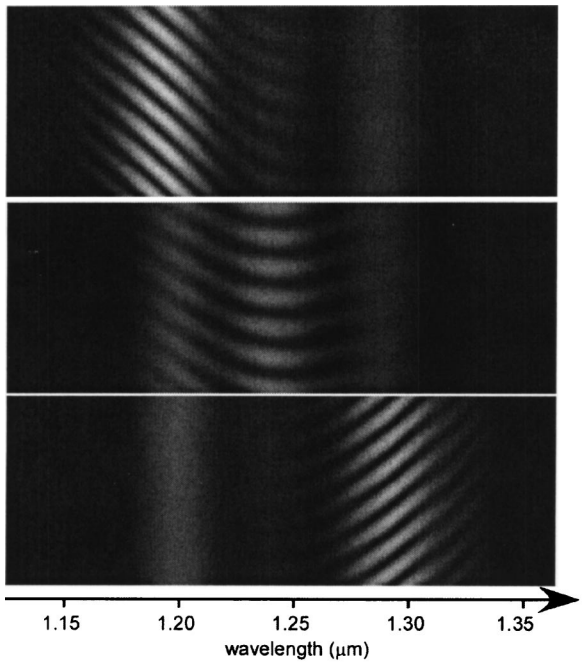

Fig. 10. Spectral interferograms that correspond to the reference pulse centered at (top to bottom) 1207, 1248, and 1295 nm.

To further test the reconstruction procedure we used two sets of interferograms, the first one corresponding to curves 1, 3, 5, 7, 9 and 11 of Fig. 9 and second one corresponding to curves 2, 4, 6, 8, and 10. The FWHM of the reference spectrum was ~38 nm; therefore each set covered more than 200 nm of signal spectrum with sufficient overlap between consecutive interferograms to permit accurate reconstruction of the complete spectral phase function. As can be seen from Figs. 11 and 12, the spectral and temporal domain data reconstructed from these two sets, which are shown by dashed and solid curves, respectively, demonstrate good agreement.

The spectral intensity and phase of the signal are shown in Fig. 11. The spectral phase shape exhibits strong nonlinearity as a result of self-phase modulation. The temporal shape of the signal (Fig. 12) exhibits a multiple-peaked structure and is found in agreement with the well-known phenomenon of pulse splitting in a bulk transparent nonlinear medium.[32,33] Pulse splitting occurs as a result of the interaction of self-focusing, self-phase modulation, and dispersion and is characteristic only for short-pulse propagation in a bulk medium (as opposed to propagation in a fiber, from which self-focusing is absent). The profile of the generated signal varies as a function of the medium's nonlinearity and dispersion as well as with the parameters of the input pulse.[34–36] A detailed analysis of this effect is, however, outside the scope of this paper.

6. CONCLUSIONS

In this paper we have described an approach to tunable single-pulse spectral phase detection based on interference between the pulses from two optical parametric amplifiers pumped by the same ultrafast amplified source. The approach combines several useful features. The use of a linear photodetector favors the detection of signals with moderate power. Independent tuning of the reference pulse wavelength permits detection of the spectral phase of broadband signals, and single-pulse operation

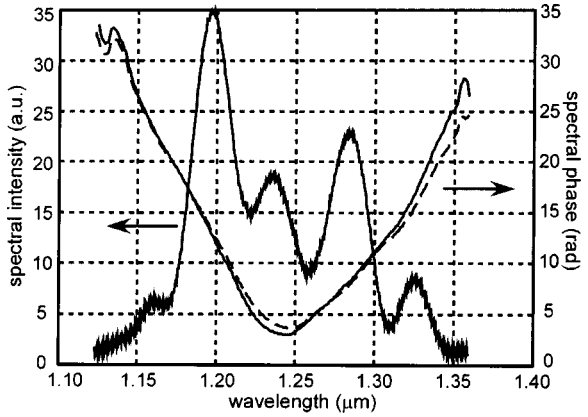

Fig. 11. Spectral intensity and phase of a nonlinearly modulated signal. Solid and dashed curves show functions extracted from two different sets of interferograms.

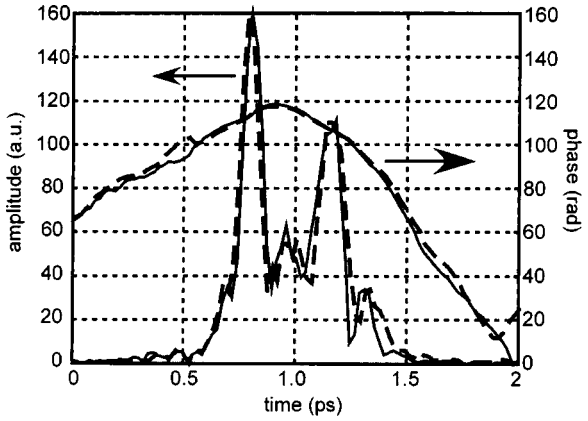

Fig. 12. Temporal amplitude and phase of the modulated signal. Solid and dashed curves show functions extracted from two different sets of interferograms.

permits revealing and investigating phase and intensity fluctuations in the signal. We expect that our approach will be useful for investigation and optimization of supercontinuum generation as well as for pulse compression and applications that require adaptive pulse shaping. As was mentioned in Section 1, strictly speaking the measurement of the complete spectral phase function is not single-shot based, as several shots with the reference tuned to different wavelengths are necessary. However, when fluctuations in the output signal are present, by monitoring the input intensity and the spectrum of the output signal one can find matching interferograms that would permit reconstruction of the complete spectral phase. An alternative way to do this, which will permit broadband phase detection in a single shot, is to use a reference pulse with a broader bandwidth. Such a pulse could be achieved in principle by use of a noncollinear parametric amplifier (NOPA).[37,38] Indeed, sub-10-fs signal pulses with bandwidths of more than 250 nm in the visible region have been generated from a NOPA pumped by the second harmonic of a Ti:sapphire regenerative amplifier (400 nm).[39] Therefore, provided that a single-pulse characterization of the NOPA signal pulse is made, the NOPA should permit true single-pulse detection of a broadband signal in the visible. The use of the idler pulse to cover the near-infrared range near 1.5 μm, however, requires a complicated optical setup to compensate for angular dispersion of the idler.[40] Therefore we believe that a tunable reference approach to phase detection is beneficial in the infrared owing to the relative simplicity of the system, provided that the generated nonlinear signal does not exhibit pulse-to-pulse fluctuations. The presence of the fluctuations in a tunable reference approach will require taking large amounts of data and a significantly more-complicated reconstruction procedure, as mentioned above. In this case utilizing the more-complicated optical setup of a mid-infrared NOPA could be desirable.

ACKNOWLEDGMENTS

This research has been supported by the Defense Advanced Research Projects Agency, the National Science Foundation, the U.S. Air Force Office of Scientific Research, and Applied Micro Circuits Corporation. D. Panasenko gratefully acknowledges the support of the Fannie and John Hertz Foundation.

*Current address, Optical Sciences Center, University of Arizona, 1630 E. University Boulevard, Tucson, Arizona 85721. E-mail, dpanasenko@optics.arizona.edu.

REFERENCES

1. I. G. Koprinkov, A. Suda, and K. Midorikawa, "Interference between stimulated Raman scattering and self-phase modulation in pressurized methane in highly transient femtosecond pump regime," Opt. Commun. **174**, 299–304 (2000).
2. M. Asobe, K. Suzuki, T. Kanamori, and K. Kubodera, "Nonlinear refractive index measurement in chalcogenide-glass fibers by self-phase modulation," Appl. Phys. Lett. **60**, 1153–1154 (1992).
3. R. R. Alfano, J. I. Gersten, G. A. Zawadzkas, and N. Tzoar, "Self-phase-modulation near electronic resonances of a crystal," Phys. Rev. A **10**, 698–708 (1974).
4. V. P. Kalosha and J. Herrmann, "Self-phase modulation and compression of few-optical-cycle pulses," Phys. Rev. A **62**, 011804 (2000).
5. J. A. R. Williams, I. Bennion, and L. Zhang, "The compression of optical pulses using self-phase-modulation and linearly chirped Bragg-gratings in fibers," IEEE Photonics Technol. Lett. **7**, 491–493 (1995).
6. V. Petrov, W. Rudolph, and B. Wilhelmi, "Compression of high-energy femtosecond light pulses by self-phase modulation in bulk media," J. Mod. Opt. **36**, 587–595 (1989).
7. D. Anderson, M. Lisak, and T. Reichel, "Importance of self-phase modulation for amplitude- and phase-modulated coherent optical transmission systems: a comparison," Opt. Lett. **13**, 285–287 (1988).
8. B.-E. Olsson and D. J. Blumenthal, "Pulse restoration by filtering of self-phase modulation broadened optical spectrum," J. Lightwave Technol. **20**, 1113–1117 (2002).
9. G. Veith, "Useful and detrimental aspects of self-phase modulation in fiber optical applications," Fiber Integr. Opt. **7**, 205–215 (1988).
10. S. A. Diddams, D. J. Jones, J. Ye, T. Cundiff, J. L. Hall, J. K. Ranka, R. S. Windeler, R. Holzwarth, T. Udem, and T. W. Hänsch, "Direct link between microwave and optical frequencies with a 300-THz femtosecond laser comb," Phys. Rev. Lett. **84**, 5102–5105 (2000).
11. I. Hartl, X. D. Li, C. Chudoba, R. K. Hganta, T. H. Ko, J. G. Fujimoto, J. K. Ranka, and R. S. Windeler, "Ultrahigh-resolution optical coherence tomography using continuum generation in an air–silica microstructure optical fiber," Opt. Lett. **26**, 608–610 (2001).
12. J. Kasparian, M. Rodriguz, G. Mejean, J. Yu, E. Salmon, H. Wille, R. Bourayou, S. Frey, Y.-B. Andre, A. Mysyrowicz, R. Sauerbrey, J.-P. Wolf, and L. Woste, "White-light filaments for atmospheric analysis," Science **301**, 61–64 (2003).
13. D. J. Kane and R. Trebino, "Single-shot measurement of the intensity and phase of an arbitrary ultrashort pulse by using frequency-resolved optical gating," Opt. Lett. **18**, 823–825 (1993).
14. C. Iaconis and I. A. Walmsley, "Spectral phase interferometry for direct electric-field reconstruction of ultrashort optical pulses," Opt. Lett. **23**, 792–794 (1998).
15. D. Panasenko and Y. Fainman, "Single-shot sonogram generation for femtosecond laser pulse diagnostics by use of two-photon absorption in a silicon CCD camera," Opt. Lett. **27**, 1475–1477 (2002).
16. C. L. Froehly, A. Lacourt, and J. C. Vienot, "Time impulse response and time frequency response of optical pupils. Experimental confirmations and applications," Nouv. Rev. Opt. **4**, 183–196 (1973).
17. Y. Weiguo, M. R. Fetterman, J. C. Davis, and W. S. Warren, "Spectral interference measurement of nonlinear pulse propagation dynamics in optical fibers," Opt. Lett. **25**, 22–24 (2000).
18. C. X. Yu, M. Margalit, E. P. Ippen, and H. A. Haus, "Direct measurement of self-phase shift due to fiber nonlinearity," Opt. Lett. **23**, 679–681 (1998).
19. D. N. Fittinghoff, J. L. Bowie, J. N. Sweetser, R. T. Jennings, M. A. Krumbugel, K. W. DeLong, R. Trebino, and I. A. Walmsley, "Measurement of the intensity and phase of ultraweak, ultrashort laser pulses," Opt. Lett. **21**, 884–886 (1996).
20. S. E. Putilin, V. L. Bogdanov, G. V. Lukomsky, M. V. Smirnov, Yu. A. Cherkasov, and Yu. T. Mazurenko, "Spectral holography of pico- and nano-second optical pulses," Opt. Laser Technol. **28**, 285–290 (1996).
21. S. E. Putilin, G. V. Lukomsky, M. V. Smirnov, and Yu. T. Mazurenko, "Recording, reproduction, and recognition of time signals by a spectral-holography method," J. Opt. Technol. **64**, 292–299 (1997).
22. A. P. Kovacs, K. Osvay, Z. Bor, and R. Szipocs, "Group delay measurement on laser mirrors by spectrally resolved white-light interferometry," Opt. Lett. **20**, 788–790 (1995).
23. D. Meshulach, D. Yelin, and Y. Silberberg, "Real-time

spatial-spectral interference measurement of ultrashort optical pulses," J. Opt. Soc. Am. B **14**, 2095–2098 (1997).
24. C. Dorrer and I. A. Walmsley, "Simple linear technique for the measurement of space–time coupling in ultrashort optical pulses," Opt. Lett. **27**, 1947–1949 (2002).
25. A. M. Weiner, J. P. Heritage, and E. M. Kirschner, "High-resolution femtosecond pulse shaping," J. Opt. Soc. Am. B **5**, 1563–1572 (1988).
26. P. Baum, S. Lochbrunner, J. Piel, and E. Riedle, "Phase-coherent generation of tunable visible femtosecond pulses," Opt. Lett. **28**, 185–187 (2003).
27. A. M. Weiner, "Femtosecond pulse shaping using spatial light modulators," Rev. Sci. Instrum. **71**, 1929–1960 (2000).
28. D. Panasenko and Y. Fainman, "Interferometric correlation of infrared femtosecond pulses with two-photon conductivity in a silicon CCD," Appl. Opt. **41**, 3748–3752 (2002).
29. W. Rudolph and J.-C. Diels, *Ultrashort Laser Pulse Phenomena: Fundamentals, Techniques, and Applications on a Femtosecond Time Scale* (Academic, San Diego, Calif., 1996).
30. J. C. M. Diels, J. J. Fontaine, I. C. Mcmichael, and F. Simoni, "Control and measurement of ultrashort pulse shapes (in amplitude and phase) with femtosecond accuracy," Appl. Opt. **24**, 1270–1282 (1985).
31. D. N. Nikogosyan, *Properties of Optical and Laser-Related Materials* (Wiley, New York, 1997).
32. P. Chernev and V. Petrov, "Self-focusing of short light pulses in dispersive media," Opt. Commun. **87**, 28–32 (1992).
33. J. E. Rothenberg, "Pulse splitting during self-focusing in normally dispersive media," Opt. Lett. **17**, 583–585 (1992).
34. S. A. Diddams, H. K. Eaton, A. A. Zozulya, and T. S. Clement, "Amplitude and phase measurements of femtosecond pulse splitting in nonlinear dispersive media," Opt. Lett. **23**, 379–381 (1998).
35. J. K. Ranka, R. W. Schirmer, and A. L. Gaeta, "Observation of pulse splitting in nonlinear dispersive media," Phys. Rev. Lett. **77**, 3783–3786 (1996).
36. M. Trippenbach and Y. B. Band, "Dynamics of short-pulse splitting in dispersive nonlinear media," Phys. Rev. A **56**, 4242–4253 (1997).
37. T. J. Driscoll, G. M. Gale, and F. Hache, "Ti:sapphire second-harmonic-pumped visible range femtosecond optical parametric oscillator," Opt. Commun. **110**, 638–644 (1994).
38. G. M. Gale, F. Hache, and M. Cavallari, "Broad-bandwidth parametric amplification in the visible: femtosecond experiments and simulations," IEEE J. Sel. Top. Quantum Electron. **4**, 224–229 (1998).
39. G. Gerullo, M. Nisoli, S. Stagira, and S. De Silvestri, "Sub-8-fs pulses from an ultrabroadband optical parametric amplifier in the visible," Opt. Lett. **23**, 1283–1285 (1998).
40. A. Shirakawa, I. Sakane, and T. Kobayashi, "Pulse-front-matched optical parametric amplification for sub-10-fs generation tunable in the visible and near infrared," Opt. Lett. **23**, 1292–1294 (1998).